RESEARCH ARTICLE

Identification of monoamine oxidase inhibitor from phytoconstituents of *Nardostachys jatamansi*: An *in-silico* study

[§]Sushmita Bhowmick[1], [§]Souvik Chakraborty[1], Sourav Pakrashy[2], Tawsif Al Arian[3], Rumdeep Kaur Grewal[4], Tarasankar Maiti[1*]

ABSTRACT

Background: Parkinson's disease is a common neurodegenerative disorder affecting older adults. It is characterized by symptoms such as poor balance, tremors, muscle rigidity, and difficulty coordinating movement. These clinical features arise primarily from the loss of dopamine-producing neurons in the central nervous system, where monoamine oxidase plays a key role in degrading dopamine. This study aims to discover potential monoamine oxidase inhibitors from *Nardostachys jatamansi* that may help slow dopamine degradation. *Materials and methods:* Phytoconstituents from the root of *Nardostachys jatamansi* were identified using the IMPPAT database, and SDF files of 25 phytoconstituents were obtained from the PubChem database. *Results:* After ADMET screening and docking analysis, two compounds, namely Pinoresinol and Virolin, were selected for MD simulations. Among the pinoresinol and virolin, pinoresinol showed a higher binding affinity in molecular docking and MD simulations. *Conclusion:* This study demonstrates that pinoresinol exhibits potent inhibitory activity against MAO-B.

Keywords: Monoamine Oxidase B (MAO-B), Parkinson's disease, *Nardostachys jatamansi*, Dopamine, Molecular docking, IMPPAT database.

Indian Journal of Physiology and Allied Sciences (2026); DOI: 10.55184/ijpas.v78i01.586 **ISSN:** 0367-8350 (Print)

INTRODUCTION

Parkinson's disease (PD) is the second most common neurodegenerative disorder worldwide after Alzheimer's[1]. Prevalence of PD is increasing with age, and PD affects 1% of the population above 60 years old.[2] This neurological disease has affected about 6.1 million people around the world in 2016.[3] By 2050, PD will have become a significant public health challenge, with approximately 25.2 million people likely to be affected worldwide.[4] In Parkinson's disease, dopaminergic neurons within the substantia nigra pars compacta (SNc) gradually degenerate, leading to reduced dopamine levels in the caudate putamen[5]. A decrease in dopamine levels in the CNS in PD is associated with several motor disorders, including tremor, bradykinesia, postural instability, and muscle rigidity.[6]

Pathophysiology of PD involves several enzymes, including tyrosine hydroxylase, catechol-O-methyltransferase (COMT), and monoamine oxidase B (MAO-B). PD treatment primarily focused on symptomatic management. Levodopa, a dopamine precursor, can cross the blood-brain barrier (BBB) and is commonly used for symptomatic treatment of PD. However, long-term use of levodopa can induce motor complications, including dyskinesia and on-off fluctuations.[7] MAO-B inhibitors can act as an adjuvant to levodopa by reducing dopamine degradation in the central nervous system, thereby increasing levodopa effectiveness and reducing motor fluctuations [8,9]. *Nevertheless, significant advancements have been made in the treatment of PD in recent years, but PD remains an incurable disease.*

Computer-based drug design techniques are widely used to identify novel drugs for many diseases, as they can reduce costs and time.[10] Because medicinal plants have few side effects, their extracts are used to treat many diseases. *Nardostachys jatamansi, a medicinal plant found in the Himalayan region, has been used to treat various neurological, respiratory, and cardiovascular disorders.11,12* This study aims to examine the potential active compound in the root extracts of N. jatamansi that inhibits *MAO-B.*

[1]Department of Physiology, Bhairab Ganguly College, West Bengal, India. Present address – University of Haifa, Sagol Department of Neurobiology, Mount Carmel, Haifa, Israel

[2]Department of Chemistry, Presidency University, West Bengal, India

[3]Department of Pharmacy, Jahangirnagar University, Dhaka, Bangladesh

[4]Department of Botany, Bhairab Ganguly College, West Bengal, India

[§] Joint First Author; *Corresponding Author.

***Corresponding author:** Tarasankar Maiti, Department of Physiology, Bhairab Ganguly College, West Bengal, India, Email: tmaiti@bhairabgangulycollege.ac.in

How to cite this article: Bhowmick S, Chakraborty S, Pakrashy S, Arian TA, Grewal RK, Maiti T. Identification of monoamine oxidase inhibitor from phytoconstituents of *Nardostachys jatamansi*: An *in-silico* study. *Indian J Physiol Allied Sci* 2026;78(1):26-32.

Conflict of interest: None

Submitted: 08/12/2025 **Accepted:** 24/01/2026 **Published:** 20/03/2026

MATERIALS AND METHODS

Selection of Phytochemicals

To identify the bioactive constituents in *Nardostachys jatamansi* roots, the IMPPAT (Indian Medicinal Plants Phytochemistry and Therapeutics) database was accessed. A

total of 25 phytochemicals from the root part of the medicinal plant *N. jatamansi* were identified, and the Structured data files (SDF) for the identified compounds were downloaded from the PubChem database (https://pubchem.ncbi.nlm.nih.gov/)[13]. Rasagiline, a MAO-B inhibitor, was also used as a control.

Computational Modeling of the Selected Target Protein

The three-dimensional structure of human MAO-B was generated using MODELLER (v10.4), which constructs protein models from experimentally resolved structures as templates.[14] The amino acid sequence of MAO-B was obtained from UniProt in FASTA format, and a BLASTP search against the Protein Data Bank (PDB) was then performed to identify homologous structures. Based on parameters such as sequence identity, query coverage, and E-value, four suitable templates were chosen: 1GOS, 2BK4, 2C73, and 2XFO. Templates with higher identity and lower E-values were prioritized to ensure reliable homology modeling.

MODELLER evaluates each generated structure using the Discrete Optimized Protein Energy (DOPE) scoring function, where lower scores indicate a more favorable and well-refined model with minimal steric issues. The structure with the lowest DOPE value was selected as the final model. To further validate its structural quality, a Ramachandran plot was produced using PROCHECK, a protein-structure assessment tool accessible through the SAVES 6.0 server (https://saves.mbi.ucla.edu/).[15]

Calculation of Drug-likeness Properties of Phytochemicals

All 25 phytochemicals from *N. jatamansi*, obtained from the IMPPAT database, were evaluated for drug-likeness to assess their potential as therapeutic candidates. Drug-likeness assessment was carried out using the online tool SwissADME, which analyzes key physicochemical properties.[16] Each compound was examined according to Lipinski's Rule of Five, which suggests that an orally active drug typically has a molecular weight under 500 Da, a log *p-value* below 5, fewer than 10 hydrogen-bond acceptors, fewer than five hydrogen-bond donors, and a limited number of rotatable bonds. Following this screening, the toxicity profiles of the filtered compounds were predicted using OSIRIS, an open-source platform for evaluating safety risks (https://www.organic-chemistry.org/prog/peo/)[17].

Molecular Docking Study

Molecular docking of the two selected compounds against the target protein was performed using the open-source software PyRx (version 0.8), which incorporates the docking engine AutoDock Vina.[18] The protein structure was first converted from PDB format to PDBQT format to prepare it for docking. All compounds, including the reference ligand, were energy-minimized with the help of Open Babel and subsequently converted from SDF to the PDBQT ligand format required by the docking program. A blind docking approach was employed to screen all 25 phytochemicals. For this purpose, a grid box large enough to encompass the entire protein was defined with the following center coordinates: X = 21.6713235641, Y = 137.152803233, Z = 40.6618480216, and dimensions (in Å): X = 69.6311586548, Y = 88.9644692127, Z = 116.280277464. Once docking was complete, the generated output files provided the binding affinities of each ligand along with the poses adopted during docking. Visualization and analysis of ligand–protein interactions were subsequently performed using BIOVIA Discovery Studio.

Molecular Dynamics Simulation Study

The behavior of the three complexes was studied using GROMACS version 2023.1 for molecular dynamics (MD) simulations.[19] The protein parameters were taken from the CHARMM General Force Field, while ligand topologies were generated using the SwissParam server[20]. To remove steric clashes, energy minimization was performed in vacuum using the steepest descent method for 2500 steps. The system was then solvated with the SPC water model, and Na^+ and Cl^- ions were added using the *gmx genion* tool to neutralize the overall charge.

After energy minimization, the system was equilibrated in two sequential stages before the production molecular dynamics run. The first stage involved a 100-picosecond NVT equilibration, during which temperature, particle number, and volume were stabilized, allowing the system to be gradually heated to 300 K. This was followed by a 100-picosecond NPT equilibration to stabilize temperature, particle number, and pressure, ensuring that the system reached an appropriate density.

Throughout all simulations, covalent bonds within the protein were constrained to maintain structural stability. These constraints also limited the motion of surrounding water molecules, thereby reducing the overall entropy of the system. Temperature regulation was achieved using the v-rescale thermostat, while the Parrinello–Rahman barostat maintained pressure, with both controls applied during the 100-ps equilibration periods.[21] The LINCS algorithm was used to fix covalent bond lengths, and long-range electrostatic interactions were computed using the Particle-Mesh Ewald (PME) method.

Before solvation, the system underwent 2,500 steps of steepest-descent vacuum minimization to eliminate steric clashes. The structure was then solvated with the SPC water model, and sodium and chloride ions were introduced to neutralize the system; ion placement was performed using the *gmx genion* utility.

Once the system was fully prepared and electrically balanced, production molecular dynamics simulations were initiated following completion of the NVT and NPT equilibration phases. These equilibration steps ensured stable thermodynamic conditions and proper system relaxation prior to the main simulation.

The root mean square deviation (RMSD) is calculated as:

$$RMSD_X = \sqrt{\frac{1}{N}\sum_{I=1}^{N}\left(r_i'(t_x)\right) - r_i(t\_ref))^2}$$

Where N is the number of selected atoms.
The reference time (t_ref) is usually set to the first frame (*t = 0*). The positions of the chosen atoms in frame x, after alignment with the reference frame, are denoted as r'. Frame x corresponds to the simulation time t_x.
All trajectory frames from the molecular dynamics (MD) simulation were carefully analyzed. RMSD was calculated to compare the structure at the start of the simulation with that of all subsequent frames throughout the MD run. The trajectory data were analyzed using XmGrace.[22] For each system, a 20-nanosecond production run was performed following equilibration.

RESULTS

Modeling of Protein structure and validation

For the modeled protein structure (qseq1.B99990002), 94.2% of the amino acid residues were located in the most favored regions of the Ramachandran plot. An additional 4.9% of residues were found in the allowed regions, while only 0.2% appeared in the generously allowed regions. The protein model also contained 42 glycine and 29 proline residues, as presented in Figure 1.

Drug likelihood analysis

The pharmacokinetic and physicochemical properties of 25 phytochemicals were assessed to evaluate their drug-likeness. Since the aim of this study was to identify compounds capable of crossing the blood–brain barrier, both Lipinski's rule of five and specific brain penetration filters were applied. Out of the 25 compounds, 20 satisfied these criteria. The toxicity of these 20 candidates was then analyzed using OSIRIS software to screen for potential mutagenic, tumorigenic, or other harmful effects. Among them, only two compounds – Virolin and Pinoresinol – passed all evaluations without any violations. Their drug-likeness profiles, further examined using SwissADME, are presented in Table 1.

Molecular Docking Assessment

A molecular docking study is a computational approach that helps predict binding affinity to the target protein in a docked complex. Two compounds, namely Virolin and Pinoresinol, along with the control drug rasagiline, were docked into the modeled protein using PyRx (version 0.8). To this end, a blind docking approach was employed (Table 2).

Visualization of the Docked complex

The docked complex of virolin and pinoresinol with the MAO-B protein was visualized for studying the interactions of the ligand with the amino acid residues of the protein (Figure 2).

Molecular Dynamics Simulations

In the first RMSD curve (Figure 3a), the backbone changes quickly during the first 2 ns, showing that the system is adjusting to its initial structure. The RMSD then rises to about 0.8 nm around 8 ns, indicating noticeable structural

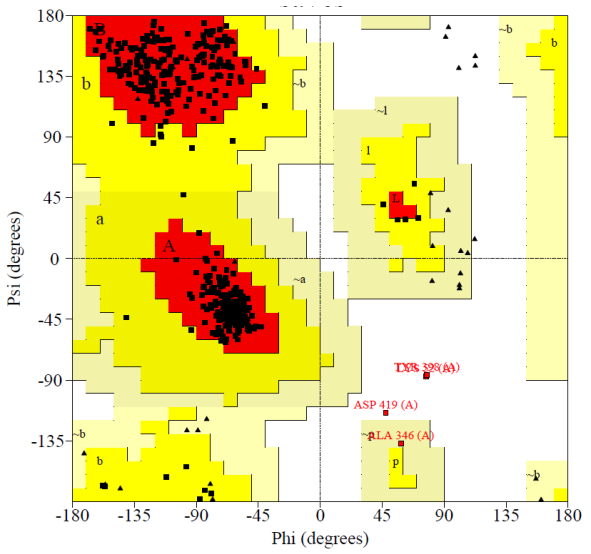

Figure 1: Ramachandran plot for modelled MAO-B protein. Triangles represent glycine residues, and proline is represented as 'p'

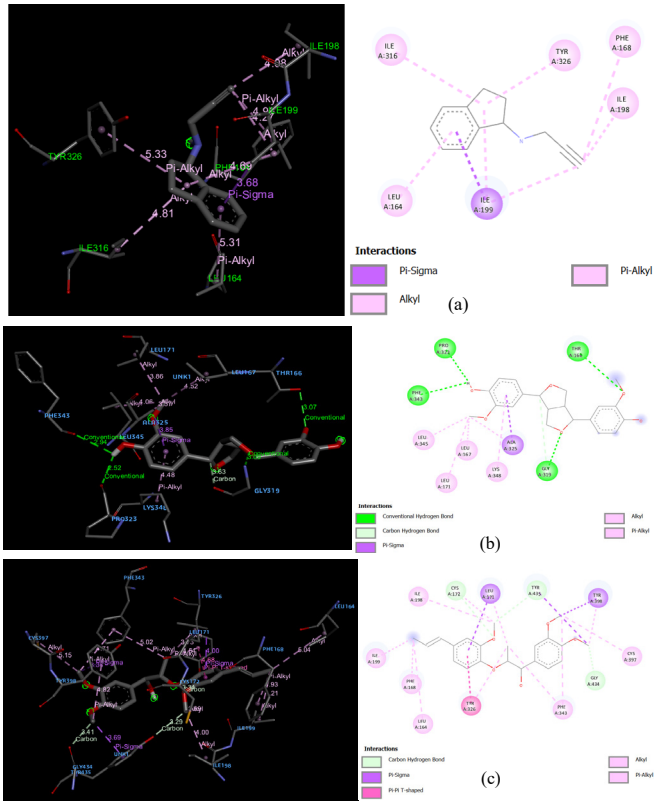

Figure 2: Three-dimensional and two-dimensional interaction of MAO-B with Rasagiline (a), Pinoresinol (b) and virolin (c)

Table 1: Evaluation of drug likeness features using SwissADME

Virolin		*Pinoresinol*	
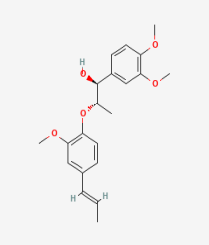	Molecular weight (g/mol) = 358.43 XLogp = 4.09 Hydrogen bond donor = 1 Hydrogen bond acceptor = 5 BBB Permeant = Yes	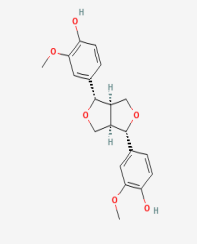	Molecular weight (g/mol) = 358.39 XLogp = 2.28 Hydrogen bond donor = 2 Hydrogen bond acceptor = 6 BBB Permeant = Yes

rearrangements. After this, it slowly decreases and levels off near 0.5 to 0.55 nm after 15 ns, suggesting the backbone becomes stable and well-equilibrated..The stability of protein–ligand complexes with pinoresinol and virolin was evaluated through backbone RMSD analysis over a 20 ns molecular dynamics trajectory (Figure 3b). Both complexes exhibited an initial rise in RMSD during the equilibration phase (0–2 ns), after which their trajectories diverged in terms of stability and fluctuation patterns. The Pinoresinol–protein complex (black trace) stabilized at higher RMSD values (average ≈ 0.64 nm after equilibration) but with relatively small fluctuations (standard deviation ≈ 0.06 nm). This indicates that, although the complex underwent a larger initial conformational adjustment, it reached and maintained a more consistent structural state throughout the simulation. In contrast, the Virolin–protein complex (red trace) showed a lower mean RMSD (≈ 0.53 nm) but considerably larger fluctuations (standard deviation ≈ 0.10 nm). The coefficient of variation was nearly twice that of pinoresinol, suggesting that the Virolin complex, although closer to the starting conformation, exhibited greater conformational flexibility and lower structural stability along the trajectory. Taken together, these results suggest that pinoresinol forms the more stable complex with the protein backbone, as reflected by its reduced RMSD variability, while Virolin binding is characterized by greater conformational instability despite a lower average RMSD.

Root-mean-square fluctuations (RMSF) indicate the flexibility of protein residues during the study. The first RMSF graph (Figure 4a) shows low fluctuations for most residues, indicating a stable protein core. A sharp increase in RMSF at the C-terminal region reveals high flexibility or disorder, suggesting this terminal segment is structurally unstable compared to the rest of the protein. Both ligands, pinoresinol (black) and virolin (red) show low fluctuations (<1 nm) across most residues, indicating structural stability. However, significant differences emerge at the C-terminal region (around residue 480 onward), where Virolin induces a sharp rise in fluctuations exceeding 6 nm, while pinoresinol shows only a modest increase (~1.5 nm). This suggests that virolin binding destabilizes and enhances flexibility in the terminal region, whereas pinoresinol maintains overall structural rigidity and stability, potentially leading to different functional consequences for protein dynamics (Figure 4b).

Figure 5a shows the total solvent accessible surface area (SASA) of the protein as a function of time. The gradual decrease in SASA indicates progressive compaction of the

Table 2: The binding affinity of the compounds, including the control drug

Name of the compound	*PubChem Id*	*Binding affinity score (kcal/mol)*
Rasagiline (control)	3052776	-7.3
Virolin	6440407	-9.2
Pinoresinol	73399	-8.3

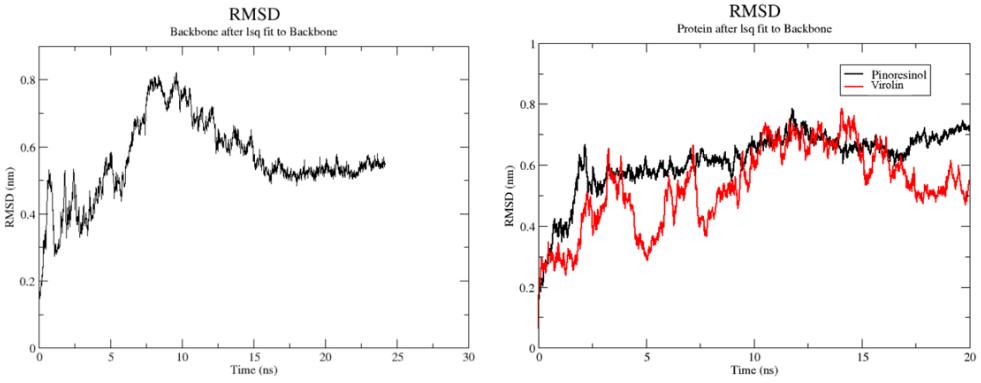

(a) (b)

Figure 3: (a) Root mean square deviation (RMSD) of protein (MAO-B) and control drug (rasagiline). (b) RMSD of pinoresinol (represented in black) and virolin (represented in red)

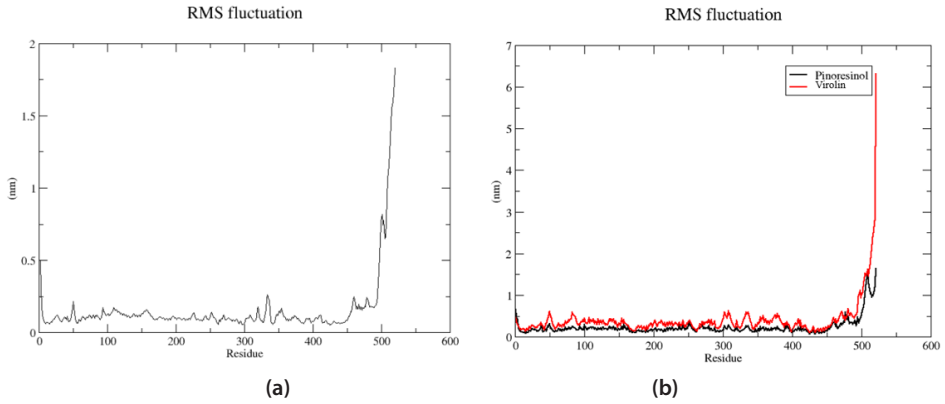

Figure 4: (a) Root mean square fluctuations (RMSF) curve for MAO-B protein and rasagiline (control drug). (b) RMSF of pinoresinol (represented in black) and virolin (represented in red)

protein structure during the simulation, while the fluctuations reflect normal breathing motions as the protein adjusts and stabilizes in the solvent environment. The SASA plot (Figure 5b) shows fluctuations in solvent exposure for pinoresinol (black) and virolin (red) complexes. Both start around ~260 nm^2, but Virolin exhibits greater variability throughout the simulation, occasionally dipping below 250 nm^2 and peaking above 270 nm^2, indicating higher conformational dynamics. Pinoresinol, by contrast, maintains more consistent SASA values, stabilizing between 255 to 265 nm^2. Toward the end of the trajectory, virolin trends toward reduced SASA, suggesting increased compactness, while pinoresinol preserves steady solvent exposure. Overall, pinoresinol stabilizes the protein conformation, whereas virolin induces greater fluctuations and conformational rearrangements.

The first figure (Figure 6a) shows the number of hydrogen bonds as a function of time. The flat line at zero throughout the simulation indicates that no hydrogen bonds were formed or maintained during the entire trajectory, suggesting an absence of stable hydrogen-bond interactions in this system. The hydrogen-bond analysis (Figure 6b) reveals clear differences between pinoresinol (black) and virolin (red). Virolin forms more stable and consistent hydrogen bonds, often maintaining 2 to 3 bonds throughout the simulation, with occasional peaks up to 4. This indicates stronger and more persistent interactions with the protein. In contrast, Pinoresinol exhibits fewer and less stable hydrogen bonds, fluctuating between 0 and 2, suggesting weaker or transient interactions. The stability of hydrogen bonding in virolin may contribute to stronger binding affinity and structural stabilization. In contrast, pinoresinol's fewer interactions reflect a less stable binding mode within the protein active site.

DISCUSSION

Parkinson's disease is a progressive neurodegenerative disorder associated with the degeneration of dopaminergic neurons, leading to motor dysfunctions such as tremors, bradykinesia, and postural instability. One of the key biochemical pathways that is affected in PD is the oxidative degradation of dopamine by MAO-B. Increased MAO-B activity catalyzes dopamine catabolism, thereby increasing

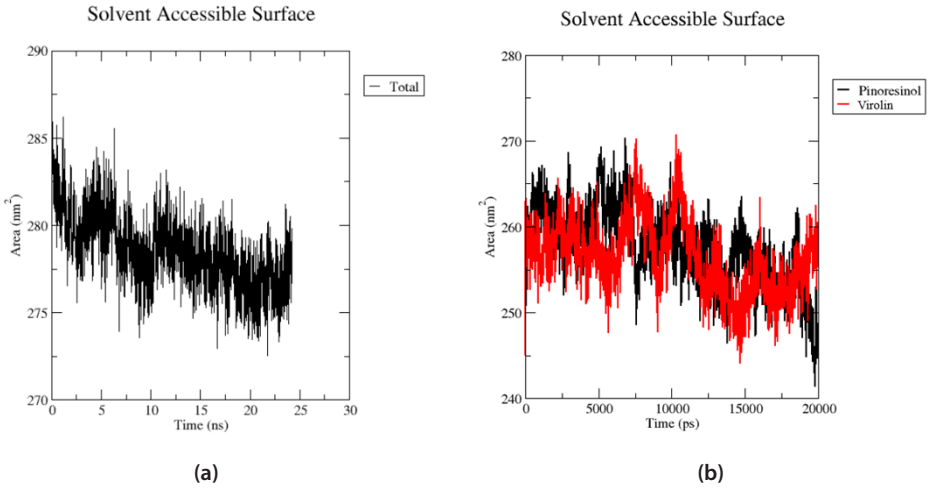

Figure 5: (a) Solvent accessible surface area (SASA) of the MAO-B protein complexed with the control drug (rasagiline). (b) SASA plot for pinoresinol (represented in black) and virolin (represented in red)

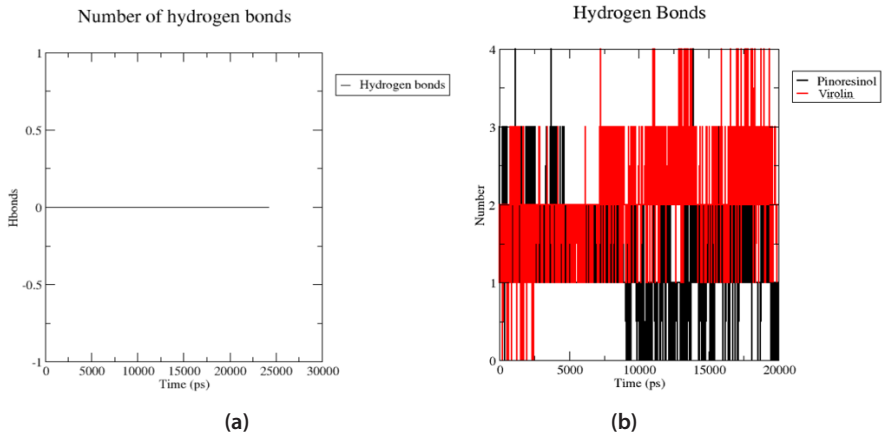

Figure 6: (a) Hydrogen bond analysis between the MAO-B protein complexed with rasagiline (control drug). (b) Hydrogen bond analysis between ligands and active site residues of the complexes of pinoresinol (represented in black) and virolin (represented in red)

oxidative stress and neuronal injury, worsening motor symptoms associated with the disease. In this study, we aimed to identify potential MAO-B inhibitors from *N. jatamansi* for the proper management of PD. MAO-B inhibitors are an essential class of drugs mainly used to treat neurodegenerative diseases such as PD.[23] This isoform of the MAO enzyme can catalyze dopamine and is highly expressed in the striatum and basal ganglia.[24] By inhibiting MAO-B, dopamine levels can be preserved, reducing oxidative damage and slowing neurodegeneration. Natural compounds have become a focus for developing MAO-B inhibitors due to their potential safety and multi-target effects.[25]

Our findings are consistent with previous reports that lignans such as pinoresinol may possess neuroprotective properties.[26] Inhibition of MAO-B may increase dopamine levels and cause oxidative damage to neurons. According to our study, pinoresinol can be used as an inhibitor of MAO-B.[27] Our study is likely the first to propose pinoresinol from the root of N. jatamansi as a promising candidate for inhibiting MAO-B in the management of PD. Further studies should focus on *in-vitro* MAO-B inhibition and *in-vivo* testing in mouse and rat PD models. Our study also has limitations, including a small sample size of potential plant-derived phytoconstituents in the present study, as it is entirely computational-based; *in-vitro* and *in-vivo* validation is required. Plant-derived MAO-B inhibitors could reduce the side effects associated with the synthetic inhibitors currently used in clinical practice. ADMET analysis was applied to the virtual screening of bioactive compounds from the root parts of N. jatamansi. Among the phytoconstituents, 2 compounds were identified, namely pinoresinol and virolin, based on ADMET and molecular docking analysis. Molecular dynamic simulation study performed on pinoresinol and virolin showed that the pinoresinol-bound protein complex was the most stable during simulation. MD simulation analysis and the significant binding affinity of pinoresinol with the protein indicate its potential as an inhibitor. Detailed docking analyses revealed that pinoresinol forms several stabilizing interactions, including hydrogen bonds and hydrophobic contacts with amino acids at the MAO-B active site. Pinoresinol has 2 hydrogen-bond donors and 6 hydrogen-bond acceptors according to SwissADME, which are favorable properties for future drug development.

CONCLUSION

The study aims to identify a potential compound from the root extracts of N. jatamansi, as reported in the Indian Medicinal Plants, Phytochemistry, and Therapeutics database, that inhibits MAO-B. The SDF files for all 25 phytoconstituents were retrieved from the PubChem database, and virtual screening was performed to identify lead compounds. Two phytoconstituents, Virolin (-9.2 kcal/mol) and Pinoresinol (-8.3 kcal/mol), were further studied using molecular docking followed by molecular dynamics simulations. Pinoresinol, a lignan from N. jatamansi, exhibits strong inhibitory potential against MAO-B and may serve as a promising lead compound for the treatment of PD. Future *in-vivo* and *in-vitro* studies will determine whether pinoresinol can be developed into a clinically viable alternative to existing MAO-B inhibitors.

ACKNOWLEDGEMENT

We gratefully acknowledge the valuable assistance provided by Dr. Amal Chandra Mondal, Professor, School of Life Sciences, Jawaharlal Nehru University (JNU), New Delhi, India.

CONFLICT OF INTEREST

The authors declare no conflict of interest

REFERENCES

1. Zhang H, Liu X, Liu Y, *et al*. Crosstalk between regulatory non coding RNAs and oxidative stress in Parkinson's disease. *Front Aging Neurosci*. 2022;14:975248 DOI:10.3389/fnagi.2022.975248
2. Tysnes OB, Storstein A. Epidemiology of Parkinson's disease. *J Neural Transm (Vienna)*. 2017;124(8):901-5. DOI: 10.1007/s00702-017-1686-y.

3. Bloem BR, Okun MS, Klein C. Parkinson's disease. *Lancet*. 2021;397(10291):2284-303. DOI: 10.1016/S0140-6736(21)00218-X.
4. Su D, Cui Y, He C, *et al*. Projections for prevalence of Parkinson's disease and its driving factors in 195 countries and territories to 2050: modelling of Global Burden of Disease Study 2021. *BMJ*. 2021;5: 388. DOI: 10.1136/bmj-2024-080952.
5. Surmeier DJ. Determinants of dopaminergic neuron loss in Parkinson's disease. *The FEBS J*, 2018;285(19): 3657-68. DOI: 10.1111/febs.14607
6. Alexander GE. Biology of Parkinson's disease: pathogenesis and pathophysiology of a multisystem neurodegenerative disorder. *Dialogues in clinical neuroscience*, 2004; 6(3):259–280. DOI: 10.31887/DCNS.2004.6.3/galexander.
7. Wu J., Lim, E. C., Nadkarni, et al. The impact of levodopa therapy-induced complications on quality of life in Parkinson's disease patients in Singapore. *Scientific reports*, 2019; *9*(1):9248. DOI: 10.1038/s41598-019451105.
8. Krishna R, Ali M, & Moustafa AA. Effects of combined MAO-B inhibitors and levodopa vs. monotherapy in Parkinson's disease. *Frontiers in aging neuroscience*, 2014; *6*:180. DOI: 10.3389/fnagi.2014.00180.
9. Tan YY, Jenner P, & Chen S. D. Monoamine Oxidase-B Inhibitors for the Treatment of Parkinson's Disease: Past, Present, and Future. *J. of Parkinson's dis*, 2022; *12*(2):477–493. DOI: 10.3233/JPD-212976
10. Gu R, Wu F, Huang Z. Role of Computer-Aided Drug Design in Drug Development. *Molecules*. 2023;28(20):7160. DOI:10.3390/molecules28207160
11. Hnamte L, Nagella P, Nizam A, Lakshmaiah VV. Phytochemicals of *Nardostachys jatamansi* as potential inhibitors of HCV E2 receptor: An *in silico* study. J App Biol Biotech. 2024;12(2):273-281. DOI: 10.7324/JABB.2024.161594
12. Pandey MM, Katara A, Pandey G, Rastogi S, Rawat AK. An important Indian traditional drug of ayurveda jatamansi and its substitute bhootkeshi: chemical profiling and antioxidant activity. *Evid Based Complement Alternat Med*. 2013;142517. DOI: 10.1155/2013/142517
13. Kim S, Thiessen PA, Bolton EE, et al. PubChem Substance and Compound databases. *Nucleic Acids Res*. 2016;44(D1): D1202-D1213. DOI:10.1093/nar/gkv951
14. Eswar N, Webb B, Marti-Renom MA, et al. Comparative protein structure modeling using Modeller. Curr protoc Bioinformatics. 2006;5 :5-6. DOI: 10.1002/0471250953.bi0506s15
15. Laskowski R.A, MacArthur M.W, Moss D.S, et al. PROCHECK: A program to check the stereochemical quality of protein structure. J of App Crystallography. 1993; 26: 283-291. DOI: 10.1107/S0021889892009944
16. Daina A, Michielin O, Zoete V. SwissADME: a free web tool to evaluate pharmacokinetics, drug-likeness and medicinal chemistry friendliness of small molecules. *Sci Rep*. 2017;7:42717. DOI:10.1038/srep42717
17. Benet L.Z, Hozey C.M, Ursu O, et al. BDDCS, the rule of 5 and drugability. Advanced Drug Del Rev. 2016; 101: 89-98. DOI: https://doi.org/10.1016/j.addr.2016.05.007
18. Eberhardt J, Santos-Martins D, Tillack A, Forli S. A. AutoDock Vina1.2.0: New docking methods, expanded force field and Python bindings. Journal of chemical information and modeling. 2021; 61: 3891-3898. DOI: https://doi.org10.1021/acs.jcim.1c00203
19. Pronk S, Páll S, Schulz R, et al. GROMACS 4.5: a high-throughput and highly parallel open source molecular simulation toolkit. *Bioinformatics*. 2013;29(7):845-854. DOI:10.1093/bioinformatics/btt055
20. Zoete V, Cuendet, MA, Grosdidier A, Michielin O. SwissParam: A Fast Force Field Generation Tool for Small Organic Molecules. *J. Comput. Chem*. 2011; *32*: 2359–2368. DOI: https://doi.org/10.1002/jcc.21816
21. Ke Q, Gong X, Liao S, Duan C, Li L. Effects of Thermostats/Barostats on Physical Properties of Liquids by Molecular Dynamics Simulations.*J.Mol.Liq*. 2022; 365: 120116. DOI: https://doi.org/10.1016/j.molliq.2022.120116
22. Knapp B, Frantal S, Cibena M, Schreiner W, Bauer P. Is an intuitive convergence definition of molecular dynamics simulations solely based on the root mean square deviation possible? *Journal of computational biology*. 2011; 18: 997-1005. DOI: https://doi.org/10.1089/cmb.2010.0237
23. Özdemir Z, Alagöz MA, Bahçecioğlu ÖF, Gök S. Monoamine Oxidase-B (MAO-B) Inhibitors in the Treatment of Alzheimer's and Parkinson's Disease. *Curr Med Chem*. 2021;28(29):6045-6065. DOI:10.2174/0929867328666210203204710
24. Osmaniye D, Kurban B, Sağlık BN, Levent S, Özkay Y, Kaplancıklı ZA. Novel Thiosemicarbazone Derivatives: In Vitro and In Silico Evaluation as Potential MAO-B Inhibitors. *Molecules*.2021;26(21):6640. Published 2021 Nov 2. DOI:10.3390/molecules26216640
25. Boulaamane Y, Ibrahim MAA, Britel MR, Maurady A. *In silico* studies of natural product-like caffeine derivatives as potential MAO-B inhibitors/$AA_{2A}R$ antagonists for the treatment of Parkinson's disease. *J Integr Bioinform*. 2022;19(4):20210027. DOI:10.1515/jib-2021-0027.
26. Giuliano C, Siani F, Mus L, Ghezzi C, Cerri S, Pacchetti B, Bigogno C, Blandini F. Neuroprotective effects of lignan 7-hydroxymatairesinol (HMR/lignan) in a rodent model of Parkinson's disease. *Nutrition*. 2020; 69: 110494. DOI: https://doi.org/10.1016/j.nut.2019.04.006
27. Liu X, Su J, Zhang J, Z Li, Huang K, Lin D, Tao E. Effects of MAO-B inhibitors in life quality of Parkinson's disease patients: A systematic review and meta-analysis. *BB Research*. 2025; 480: 115410. DOI: https://doi.org/10.1016/j.bbr.2024.115410

PEER-REVIEWED CERTIFICATION

During the review of this manuscript, a double-blind peer-review policy has been followed. The author(s) of this manuscript received review comments from a minimum of two peer-reviewers. Author(s) submitted revised manuscript as per the comments of the assigned reviewers. On the basis of revision(s) done by the author(s) and compliance to the Reviewers' comments on the manuscript, Editor(s) has approved the revised manuscript for final publication.